Ink4a and *Arf* differentially affect cell proliferation and neural stem cell self-renewal in *Bmi1*-deficient mice

Sophia W.M. Bruggeman,[1,4] Merel E. Valk-Lingbeek,[1,4] Petra P.M. van der Stoop,[1,5] Jacqueline J.L. Jacobs,[1,5] Karin Kieboom,[1] Ellen Tanger,[1] Danielle Hulsman,[1] Carly Leung,[2] Yvan Arsenijevic,[3] Silvia Marino,[2] and Maarten van Lohuizen[1,6]

[1]Division of Molecular Genetics, The Netherlands Cancer Institute, 1066 CX Amsterdam, The Netherlands; [2]Department of Pathology, Institute of Clinical Pathology, University of Zürich, 8091 Zürich, Switzerland; [3]Laboratory of Oculogenetics, Opthalmic Hospital Jules Gonin, Lausanne University, 1004 Lausanne, Switzerland.

The Polycomb group (PcG) gene *Bmi1* promotes cell proliferation and stem cell self-renewal by repressing the *Ink4a/Arf* locus. We used a genetic approach to investigate whether *Ink4a* or *Arf* is more critical for relaying *Bmi1* function in lymphoid cells, neural progenitors, and neural stem cells. We show that *Arf* is a general target of *Bmi1*, however particularly in neural stem cells, derepression of *Ink4a* contributes to *Bmi1*$^{-/-}$ phenotypes. Additionally, we demonstrate haploinsufficient effects for the *Ink4a/Arf* locus downstream of *Bmi1* in vivo. This suggests differential, cell type-specific roles for *Ink4a* versus *Arf* in PcG-mediated (stem) cell cycle control.

Supplemental material is available at http://www.genesdev.org.

Received January 19, 2005; revised version accepted May 4, 2005.

The *Bmi1* gene, originally identified as a collaborating oncogene in *c-Myc* induced lymphomagenesis, is a member of the Polycomb group (PcG) gene family of chromatin modifiers and transcriptional repressors (Haupt et al. 1991; Van Lohuizen et al. 1991). Loss of a *PcG* gene alters *Homeobox* (*Hox*) gene expression resulting in skeletal malformations (Van der Lugt et al. 1994; Akasaka et al. 1996; Core et al. 1997; Del Mar Lorente et al. 2000). However, *Hox* genes are not the only targets of PcG as the tumor suppressor locus *Cdkn2a* (hereafter *Ink4a/Arf* locus) is also negatively regulated by *Bmi1* and other PcG members (Jacobs et al. 1999; Voncken et al. 2003; Core et al. 2004; Gil et al. 2004).

[*Keywords*: *Bmi1*; *Ink4a*; *Arf*; Polycomb; stem cell development]
[4,5]These authors contributed equally to this work.
[6]Corresponding author.
E-MAIL m.v.lohuizen@nki.nl; FAX 31-20-512-2011.
Article and publication are at http://www.genesdev.org/cgi/doi/10.1101/gad.1299305.

The *Ink4a/Arf* locus codes for two proteins, p16^{ink4a} and p19^{arf} (*Ink4a* and *Arf*), by use of alternative reading frames (Serrano et al. 1993; Quelle et al. 1995). *Ink4a* and *Arf* are important players in the *retinoblastoma* (*pRB*) and *p53* pathways, respectively, and their activation results in growth arrest, senescence, or apoptosis (for review, see Sharpless and DePinho 1999; Lowe and Sherr 2003). *Bmi1*-deficient mice suffer from abnormalities of the hematopoietic and nervous system in addition to growth retardation and skeletal malformations (Van der Lugt et al. 1994). Generation of *Bmi1;Ink4a/Arf* compound mutant mice provided genetic evidence that at least part of these defects are due to derepression of the *Ink4a/Arf* locus (Jacobs et al. 1999). Interestingly, we and others have recently shown that *Bmi1* is essential for the self-renewal of hematopoietic and neural stem cells, and proliferation of cerebellar granule neuron progenitors (Lessard and Sauvageau 2003; Molofsky et al. 2003; Park et al. 2003; Iwama et al. 2004; Leung et al. 2004; Zencak et al. 2005). Loss of *Ink4a* could partially alleviate the self-renewal defect of *Bmi1*-deficient neural stem cells, implicating that inappropriate activation of the *Ink4a/Arf* locus negatively influences stem cell renewal (Molofsky et al. 2003).

However, since *Bmi1* is a potent repressor of both *Ink4a* and *Arf* it is important to discriminate which one of these genes is crucial for *Bmi1* function. Here we took advantage of the various specific knockout mouse models made for the locus. We addressed the relative contribution of *Ink4a* and *Arf* deregulation to a variety of *Bmi1*$^{-/-}$ phenotypes with emphasis on the hematopoietic and central nervous system. We reveal specific dosage effects of *Ink4a* and *Arf* in vivo, and demonstrate that *Arf* is a general target of *Bmi1* in lymphoid cells, neural progenitors, and stem cells. Importantly, particularly in neural stem cells deregulated expression of *Ink4a* contributes to the *Bmi1*-deficient phenotype, altogether highlighting differential, cell type-specific requirements for *Ink4a* versus *Arf* in *Bmi1*-mediated control of cell proliferation.

Results and Discussion

Differential effects of Ink4a *and* Arf *derepression in* Bmi1*-deficient lymphoid organs*

Bmi1$^{-/-}$ mice suffer from progressive hypoplasia of the spleen and thymus as illustrated by a large reduction in lymphocyte counts (Van der Lugt et al. 1994; Fig. 1). We have previously shown that *Ink4a/Arf* is an in vivo target of *Bmi1* in the lymphoid system (Jacobs et al. 1999). Here we investigated the impact of *Ink4a* versus *Arf* derepression on lymphocyte counts in *Bmi1*$^{-/-}$ mice. In the thymus but not in spleen, *Arf* loss gives a significantly smaller rescue than *Ink4a/Arf* loss, revealing a role for *Ink4a* restricting thymocyte growth downstream of *Bmi1* ($p < 0.01$) (Fig. 1A,C). However, loss of *Ink4a* alone does not alleviate the phenotype showing that reduction of *Arf* levels is a prerequisite (Fig. 1B,D). Lack of rescue from *Bmi1* deficiency upon *Ink4a* deletion is not unique for splenocytes. Also *Bmi1*$^{-/-}$ mouse embryonic fibroblasts (MEFs), which up-regulate p16^{ink4a} and p19^{arf} in a dose-dependent manner (Supplementary Fig. 1A), are

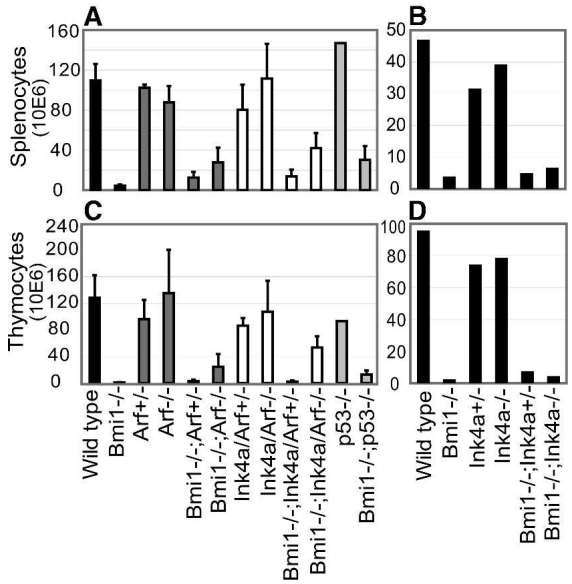

Figure 1. Differential effects of *Ink4a* and *Arf* dosage and derepression in *Bmi1*$^{-/-}$ lymphoid organs. (*A*) Splenocyte counts are dramatically reduced in *Bmi1*$^{-/-}$ mice. Heterozygosity for *Arf* or *Ink4a/Arf* partially rescues this phenotype ($p < 0.01$) but complete loss of *Arf* or *Ink4a/Arf* results in a better partial rescue. *p53* loss also induces a partial rescue. (*B*,*D*) Neither *Bmi1*$^{-/-}$ splenocyte nor thymocyte counts are significantly restored by loss of *Ink4a*. (*C*) Thymocyte counts are dramatically reduced in *Bmi1*$^{-/-}$ mice. Loss of the complete *Ink4a/Arf* locus gives a substantially better rescue than loss of *Arf* alone ($p < 0.05$). Note that heterozygosity does not lead to a rescue. *p53* loss induces a minor rescue in lymphocyte counts.

only rescued from premature senescence upon loss of *Arf* (Supplementary Fig. 1B,C). Intriguingly, in the *Bmi1*-deficient spleen but not in thymus, heterozygosity for either *Arf* or *Ink4a/Arf* alleviates the reduced cell counts to a minor yet significant extent ($p < 0.001$), indicating that specific threshold levels of *Ink4a* and *Arf* are required (Fig. 1A,C).

Similar effects occur in the composition of the splenic B-cell population. *Bmi1*$^{-/-}$ mice harbor increased thymic populations of $CD4^-CD8^-$ immature T-cells and a decreased number of splenic mature $B220^+sIg^+$ B-cells (Van der Lugt et al. 1994; Jacobs et al. 1999). Applying flow cytometry using standard T- and B-cell differentiation markers, we found that in spleen, heterozygosity for either *Arf* or *Ink4a/Arf* completely restores the relative population frequency of mature B-cells to wild-type levels (Supplementary Fig. 2A,B). In contrast in thymus, only complete loss of *Arf* or *Ink4a/Arf* results in a relative restoration of wild-type levels of immature $CD8^-CD4^-$ T-cells (Supplementary Fig. 2A,C).

Lastly, we questioned whether *Bmi1* signals to the *Arf* target *p53*. $p19^{arf}$ controls the activity of p53 by sequestering Mdm2, an E3 ubiquitin ligase for p53 (for review, see Sherr and Weber 2000). As depicted in Figure 1A,C and Supplementary Figure 1D, both lymphocyte counts and fibroblast proliferation are (partially) rescued upon *p53* deletion. Moreover, *Mdm2* overexpression rescues the impaired proliferation of *Bmi1*$^{-/-}$ MEFs as well (Supplementary Fig. 1E). This strongly suggests that at least part of the *Bmi1*$^{-/-}$ phenotypes are caused by *p53* activation through *Arf*.

Proliferation defects in Bmi1*-deficient cerebellum reflect* Ink4a *and* Arf *deregulation*

When investigating the neurological defects of *Bmi1*$^{-/-}$ mice, we recently pinpointed a reduced number of poorly proliferating cells of the cerebellar external granular layer (EGL) to be partially responsible (Leung et al. 2004). During normal early post-natal development, a wave of proliferation of cerebellar granule neuron progenitors (CGNPs) in the EGL is induced by Purkinje neuron secreted Sonic Hedgehog (Shh) (Dahmane and Ruiz-I-Altaba 1999; Wechsler-Reya and Scott 1999). In time, CGNPs differentiate and migrate inwards past the molecular layer (ML) until they reach the internal granular layer (IGL) where they reside as mature granule neurons (for review, see Wang and Zoghbi 2001). We were able to link this process to PcG by showing that *Bmi1* is a target of *Shh*, thus explaining the impaired proliferative response of *Bmi1*$^{-/-}$ CGNPs upon Shh stimulation (Leung et al. 2004). As *Bmi1*$^{-/-}$ CGNPs are still partially responsive to Shh, we proposed a model where Shh controls proliferation via at least two routes, i.e., through induction of *N-Myc/Cyclin D2* (Kenney et al. 2003) and through *Bmi1*-mediated repression of *Ink4a/Arf*.

Analysis by quantitative real-time PCR (qRT-PCR) shows that *Ink4a* and to a lesser extent *Arf* expression is increased in *Bmi1*$^{-/-}$ CGNPs and cerebella (Fig. 2A). Moreover, we demonstrate that stimulation of wild-type CGNPs with Shh leads to an induction of Bmi1 protein expression and a concomitant significant down-regulation of both *Ink4a* and *Arf* transcript levels, consistent with the idea of Shh regulating *Ink4a/Arf* through *Bmi1* (Fig. 2C,D). To assess to what extent *Ink4a* and *Arf* deregulation underlies the proliferative defects of *Bmi1*$^{-/-}$

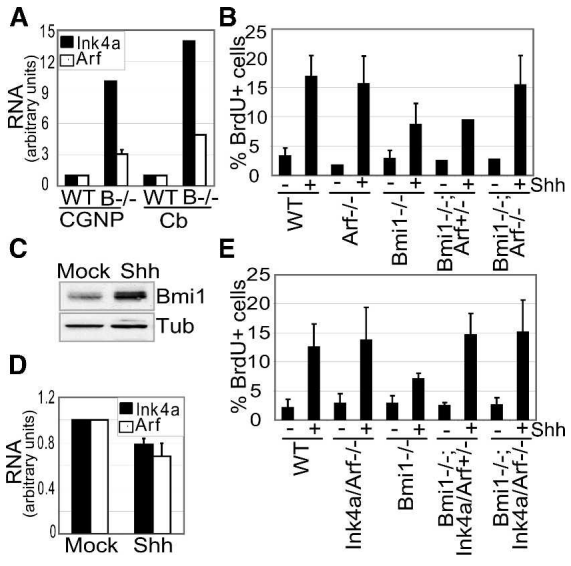

Figure 2. *Ink4a/Arf* derepression upon *Bmi1* loss prevents efficient Shh-induced CGNP proliferation. (*A*) qRT-PCR shows up-regulation of *Ink4a* and *Arf* mRNA expression in *Bmi1*$^{-/-}$ CGNPs and cerebella. (B) *Bmi1*; (Cb) cerebellum. (*B*) Reduced BrdU incorporation in *Bmi1*$^{-/-}$ CGNPs upon Shh treatment ($p < 0.001$) is rescued upon subsequent *Arf* loss ($p < 0.01$) but not by *Arf* heterozygosity. (*C*,*D*) In wild-type CGNPs, Shh treatment induces an increase in Bmi1 protein levels and a decrease in *Ink4a* ($p < 0.005$) and *Arf* ($p < 0.02$) mRNA expression. (Tub) Tubulin. (*E*) Reduced BrdU incorporation in *Bmi1*$^{-/-}$ CGNPs upon Shh treatment is rescued by *Ink4a/Arf* loss ($p < 0.05$) and *Ink4a/Arf* heterozygosity ($p < 0.03$).

CGNPs, we investigated the Shh response of *Bmi1;Arf* and *Bmi1;Ink4a/Arf* doubly deficient CGNPs and their respective controls. Notably, neither *Arf* nor *Ink4a/Arf* loss causes enhanced proliferation in absence of Shh in line with the multiple levels of regulation downstream of Shh (Fig. 2B,E). However in the context of *Bmi1* deficiency, both *Arf* loss alone and complete loss of the *Ink4a/Arf* locus rescues Shh-induced proliferation of $Bmi1^{-/-}$ CGNPs to control levels ($p < 0.05$) (Fig. 2B,E). Notably, we observe a clear effect of heterozygosity for *Ink4a/Arf* in $Bmi1^{-/-}$ CGNPs similarly to thymus (Fig. 2E).

We demonstrated earlier that loss of *Ink4a/Arf* gives a qualitative rescue of the $Bmi1^{-/-}$ cerebellar defects in vivo (Jacobs et al. 1999). Since we found that *Arf* loss fully rescued $Bmi1^{-/-}$ CGNPs in vitro, we questioned to what extent this affects in vivo proliferation of cerebellar progenitor cells. Histological analysis revealed that the reduced thickness of the $Bmi1^{-/-}$ granular layer is rescued to a similar extent in either an $Arf^{-/-}$ or $Ink4a/Arf^{-/-}$ background (Fig. 3A,B). Surprisingly, the cell density of the $Bmi1^{-/-}$ IGL is fully rescued in an $Ink4a/Arf^{-/-}$ background, but only partially in an $Arf^{-/-}$ background ($p < 0.01$) pointing at a subtle role for *Ink4a*-repression in the IGL in vivo (Fig. 3A,C). Disturbed EGL proliferation can explain multiple abnormalities of the cerebellum. Particularly later during development, granule neurons signal to Purkinje and Basket cells to create the appropriate amount of arborization (Baptista et al. 1994). However, despite proliferation substantially being restored in *Bmi1;Arf-* and *Bmi1;Ink4a/Arf*-deficient CGNPs, these mice still display neurological abnormalities. This implies that at least part of the $Bmi1^{-/-}$ cerebellar phenotype is due to defects in cell types other than CGNPs. The cerebellum originates from two germinal layers, the rhombic lip from which the CGNPs are derived, and the ventricular zone which gives birth to the molecular neurons (for review, see Wang and Zoghbi 2001). It is conceivable that *Bmi1* also plays a role in cells derived from the ventricular zone, especially since *Bmi1* is required for the self-renewal of adult neural stem cells from the subventricular zone, a closely related germinal layer of the cerebrum (see below). Indeed, we observed aberrations such as reduced cellularity of the molecular layer (Fig. 3A,D) and abnormal arborization of basket neurons in $Bmi1^{-/-}$ and $Bmi1^{-/-}$;*(Ink4a/)*$Arf^{-/-}$ cerebella (Fig. 3A). Interestingly, the reduction in ML neurons is partially rescued by *Ink4a/Arf* loss and not significantly by *Arf* loss ($p < 0.05$), suggesting a role for *Ink4a*-repression in molecular layer neurons in vivo (Fig. 3D).

Neural stem cell self-renewal critically depends on repression of Ink4a *and* Arf *by* Bmi1

A stem cell is defined as a multipotent cell capable of extensive self-renewal. For neural stem cells, multipotency means the cell can give rise to neurons and glial cells. One major neurogenic region in the adult cerebrum harboring stem cells is the subventricular zone (SVZ) of the lateral ventricle wall (for review, see Doetsch 2003). Neural stem cells isolated from the SVZ can be grown as either adherent colonies or as "neurospheres", floating clusters of stem cells and progeny (Reynolds and Weiss 1992; Morshead et al. 1994).

Recently, Molofsky et al. demonstrated that *Bmi1* is essential for the self-renewal of SVZ-derived neurospheres and that *Ink4a* repression is partially mediating this effect (Molofsky et al. 2003). Here we set out to determine whether *Arf* is required as well. Western blot analysis on wild-type and *Bmi1* knockout cerebral tissue (isolated from post-natal day 30 [P30] mice) revealed

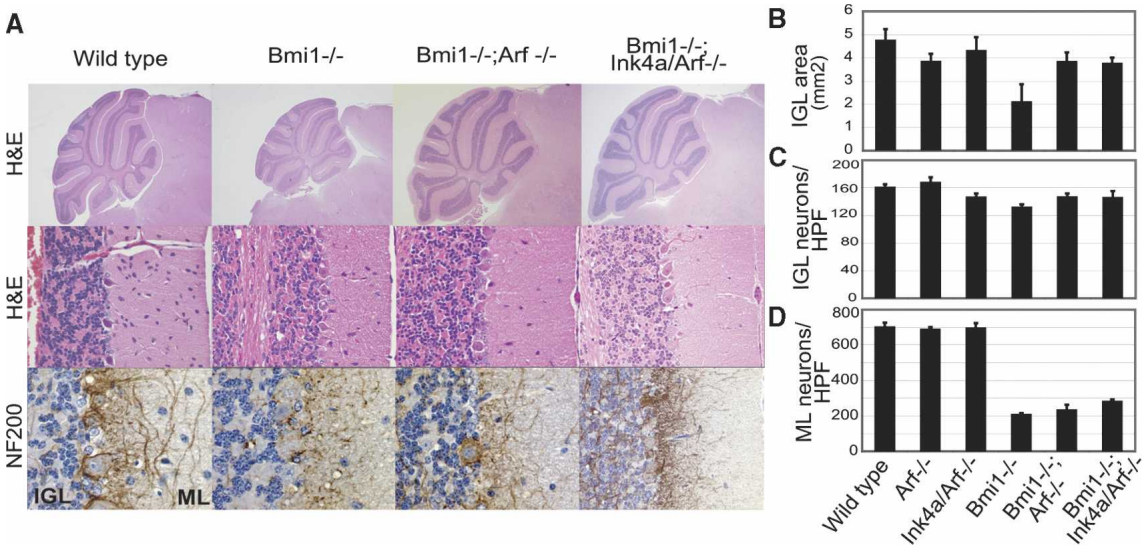

Figure 3. *Ink4a* and *Arf* differentially contribute to histological abnormalities of the $Bmi1^{-/-}$ cerebellum. (*A*) Morphological analysis of wild-type (*left* panels), $Bmi1^{-/-}$ (*middle left* panels), $Bmi1^{-/-}$;$Arf^{-/-}$ (*middle right* panels), and $Bmi1^{-/-}$;$Ink4a/Arf^{-/-}$ (*right* panels) adult cerebellum. Haematoxylin and eosin (H&E, *top* and *middle* panels) staining shows rescue of overall cerebellar size and granular layer thickness in $Bmi1^{-/-}$;*(Ink4a)*$Arf^{-/-}$ mice. (*Bottom* panels) Aberrant arborization of basket neurons (NF200 staining) is observed in all cerebella lacking *Bmi1*. Final magnification, 5× and 60×. (IGL) Internal granular layer; (ML) molecular layer. (*B*) IGL area measurements reveal similar significant rescues in $Bmi1^{-/-}$;$Arf^{-/-}$ and $Bmi1^{-/-}$;$Ink4a/Arf^{-/-}$ mice. (*C*) *Ink4a/Arf* loss induces a complete rescue of the number of $Bmi1^{-/-}$ granule neurons, whereas *Arf* loss leads to a partial rescue ($p < 0.01$). (*D*) The partial rescue in number of $Bmi1^{-/-}$ molecular layer neurons is significantly better in an *Ink4a/Arf* deficient background ($p < 0.05$) (HPF, high-power field; $n = 4$ mice).

up-regulated p16^{ink4a} expression in the *Bmi1*$^{-/-}$ brain (Fig. 4B). In addition, qRT-PCR demonstrated that alike in MEFs and cerebellum, *Ink4a* and *Arf* transcripts are up-regulated, establishing *Ink4a/Arf* as a bona fide in vivo *Bmi1* target (Fig. 4C). Next, we prepared adult SVZ neural stem cell cultures at clonal density and assured that the vast majority of primary neurospheres was derived from multipotent stem cells by staining for neuronal and glial markers (Fig. 4A, right panel). Strikingly, *Bmi1*$^{-/-}$ primary neurospheres not only form less frequently, but also differentiate less efficiently (Fig. 4A right panel) and are much smaller in size than control neurospheres (Fig. 4A [left panel], D). The latter observation suggests that proliferation within a *Bmi1*$^{-/-}$ neurosphere, reflecting the sum of cell divisions from self-renewing stem cells and their progeny, is impaired. Indeed, *Bmi1*$^{-/-}$ colonies incorporate far less BrdU than control colonies (Fig. 4F). Notably, this defect in proliferation can be rescued by both loss of *Arf* and by complete deletion of the *Ink4a/Arf* locus implicating *Arf* as an important downstream effector of *Bmi1* for stem cell and progenitor proliferation (Fig. 4A,F).

Next, we performed a neurosphere assay to specifically study stem cell self-renewal. In this assay, the capacity of a primary neurosphere to form new multipotent neurospheres after dissociation is measured. We report a dramatic decrease in the self-renewing capacity of both adult (P30) and P7-derived *Bmi1*$^{-/-}$ neurospheres in agreement with previous findings (Fig. 4E). Deletion of the *Ink4a/Arf* locus in *Bmi1*$^{-/-}$ neurospheres completely rescues this defect. Importantly, loss of *Arf* alone gives a partial rescue ($p < 0.05$), reinforcing the earlier observation that proper repression of *Ink4a* is also required for neurosphere self-renewal. This does not simply reflect a tissue culture phenomenon as is highlighted by Molofsky et al. (2005) who found that *Ink4a* loss partially restores *Bmi1*$^{-/-}$ stem cell frequency and neurogenesis in vivo. Upon induction of differentiation, all secondary neurospheres stained positive for neuron and astrocyte specific markers (data not shown). Surprisingly, there is a clear increase in both proliferation and self-renewing capacity of *Arf* and *Ink4a/Arf* deficient neurospheres compared with wild types (Fig. 4E,F). This strongly suggests that the *Ink4a/Arf* locus actively restricts self-renewing cell divisions thus playing a role in controlling the stem cell compartment. Lastly, we tested these neurospheres for long-term self-renewal as, for instance, exhaustion of hematopoietic stem cells sometimes occurs after a prolonged period of time (Park et al. 2003). However, we were able to keep *Bmi1*$^{-/-}$;*Arf*$^{-/-}$ and *Bmi1*$^{-/-}$;*Ink4a/Arf*$^{-/-}$ neurospheres in culture for at least five weekly passages, suggesting that the *Bmi1* knockout phenotype is fully reversed.

A specific subset of PcG proteins appears to regulate stem cell self-renewal and progenitor proliferation

How could PcG distinctly regulate its target genes in different cell types? Emerging studies indicate that different "flavors" of PcG complexes may exist (De Napoles et al. 2004; Kuzmichev et al. 2004). An increase in the relative amount of a PcG member such as *Bmi1*, may alter the affinity of a PcG complex towards the chromatin in such a way that for instance self-renewing divisions are favored (for review, see Valk-Lingbeek et al. 2004). Underscoring a special role for *Bmi1*, we found

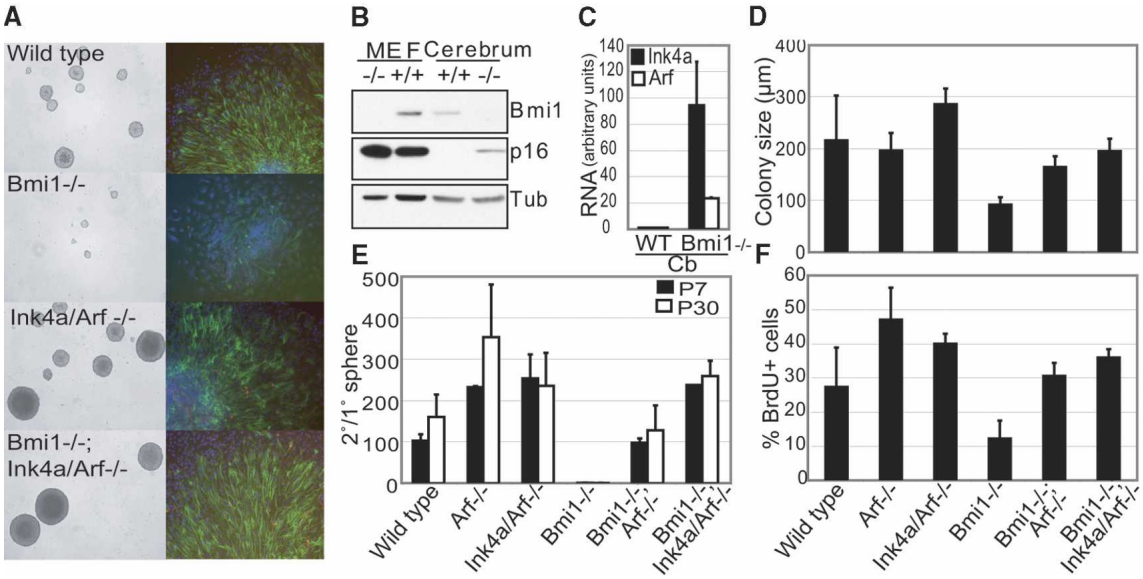

Figure 4. Accurate repression of *Ink4a* and *Arf* is required for neurosphere self-renewal. (*A*,*D*) Phase-contrast pictures (*A*, *left* panel) and diameter measurements show that *Bmi1*$^{-/-}$ neurospheres are much smaller than wild types. Loss of either *Arf* or *Ink4a/Arf* completely rescues this *Bmi1*$^{-/-}$ phenotype. (*A*, *right* panel) All primary neurospheres are multipotent. Note that *Bmi1*$^{-/-}$ spheres differentiate less efficiently (GFAP staining in green and β-tubulin-III in red). (*B*) Western blot analysis reveals increased p16^{ink4a} expression in *Bmi1*$^{-/-}$ cerebrum. (Tub) Tubulin. (*C*) qRT-PCR shows increased *Ink4a* and *Arf* mRNA expression in *Bmi1*$^{-/-}$ cerebrum. (Cb) Cerebrum. (*E*) P7- and P30-derived *Bmi1*$^{-/-}$ neurospheres are severely impaired in their self-renewal capacity. *Arf* loss alone gives a partial rescue of this phenotype ($p < 0.05$). Removal of the complete *Ink4a/Arf* locus fully restores the self-renewing ability of *Bmi1*$^{-/-}$ neurospheres. Note that loss of *Arf* or *Ink4a/Arf* in a *Bmi1*$^{+/+}$ background enhances self-renewal ($p < 0.01$). (1°) Primary; (2°) secondary. (*F*) *Bmi1*$^{-/-}$ SVZ adherent colonies incorporate less BrdU than control colonies, which is completely rescued upon loss of either *Arf* or *Ink4a/Arf*.

that loss of *Ring1a* or *M33*, PcG proteins belonging to the same complex as *Bmi1,* does not affect neurosphere self-renewal or CGNP proliferation (Supplementary Fig. 3A,B). Only loss of *Mel18*, the closest homolog of *Bmi1*, has a modest though not significant negative effect on these processes in accordance to recent observations in hematopoietic stem cells (Iwama et al. 2004).

It remains striking that lymphoid cell counts, cerebellar development, skeletal transformations, and overall body growth in *Bmi1;Ink4a/Arf* doubly deficient mice are at best partially rescued (Figs. 1, 3; Supplementary Table 1; Supplementary Fig. 4). Therefore, other *Bmi1* regulated genes must exist. In line with *Drosophila* not possessing genes resembling the *Ink4a/Arf* locus, the acquisition of PcG-mediated proliferation control likely evolved later, perhaps reflecting a demand for protection of long lasting stem cells. Candidates for additional *Bmi1* targets are the *Hox* genes. Interestingly, a subset of *Hox* genes has been implicated in mammalian brain development and control of hematopoiesis. Moreover, several *Hox* genes are differentially expressed in $Bmi1^{-/-}$ SVZ neurospheres (Molofsky et al. 2003). However, it cannot be excluded that a substantial number of additional targets exists, as PcG proteins as chromatin modifiers are known to act on large gene sets (Kirmizis et al. 2004). Altogether, we have demonstrated profound tissue and cell type specific differences in the effects of *Ink4a* versus *Arf* derepression in *Bmi1*-deficient mice. We propose a general role for *Bmi1*-mediated *Arf/p53* repression in curtailing proliferation. *Ink4a* repression on the other hand is required only in a subset of cells. Furthermore, we show haploinsufficient effects of the *Ink4a/Arf* locus in vivo selectively for certain tissues, and suggest that appropriate threshold levels of these two proteins are required to ensure proper proliferation. These observations implicate PcG proteins not only in embryonic developmental fate decisions, but also in discriminative processes between cell cycle control of stem- and more differentiated cells.

Materials and methods

Mice breeding, lymphocyte counts and flow cytometry

$Bmi1^{+/-}$ FVB or C57BL/6 mice (Van der Lugt et al. 1994) were crossed with $Ink4a/Arf^{+/-}$ FVB mice (Serrano et al. 1996), with $Arf^{+/-}$ FVB mice (Kamijo et al. 1997), with $p53^{+/-}$ FVB mice (Donehower et al. 1992), or $Ink4a^{+/-}$ C57BL/6 mice (Krimpenfort et al. 2001). In addition, *Ring1a* FVB mice (Del Mar Lorente et al. 2000), *M33* FVB mice (Core et al. 1997) and *Mel18* (mixed background) knockout mice (Akasaka et al. 1996) were used. All mice were genotyped routinely by PCR (list of primers available upon request). Multiple independent animals of the respective genotypes were assayed and all results were subjected to Student's *t*-tests and Bonferroni correction when appropriate. Preparation of cell suspensions from lymphoid organs, cell counts, and flow cytometric analyses were done as described previously (Jacobs et al. 1999).

Western blot analysis and quantitative real-time PCR

Equal amounts of protein were separated on 13% SDS-PAGE or precast gels (Invitrogen) and blotted onto Immobilon-P membranes (Amersham Biosciences). Bands were visualized using enhanced chemiluminescence (Amersham). Primary antibodies were F6 for Bmi1 (Upstate), M156 for $p16^{ink4a}$ (Santa Cruz), or R562 for $p19^{arf}$ (Abcam). Secondary antibodies were goat-anti-mouse (ZyMed) or goat-anti-rabbit (BioSource), both HRP conjugated. Total RNA was extracted using TRIZOL reagent (Invitrogen) and cDNA was prepared using Superscript II RT and oligod$(T)_n$ primers (Invitrogen). qRT-PCR was performed with 50 ng cDNA on an ABI PRISM 7000 using SYBR Green PCR mastermix (Applied Biosystems). For primer sequences and formulas, see Supplemental Material.

CGNP isolation and histology of cerebellar tissue

CGNP cultures were isolated from 7 d-old-mice and cultured according to established protocols (Wechsler-Reya and Scott 1999; Leung et al. 2004). Quantification of Shh-induced proliferation was performed as described previously (Leung et al. 2004). Immunocytochemistry was performed using mouse monoclonal anti-BrdU (DAKO) and Alexa Fluor m488 goat-anti-mouse (Molecular Probes). DAPI (Molecular Probes) was used to visualize nuclei. Immunohistochemistry and histological analysis were performed as described before (Leung et al. 2004).

Neural stem cell isolation, neurosphere proliferation, and self-renewal assays

For neural stem cell isolation and culture conditions, see Supplemental Material. To assess proliferation, primary adherent stem cell colonies were pulsed for 1 h with 1 µM BrdU (7 d after isolation). Immunocytochemistry was performed as for CGNPs. The self-renewal capacity was determined by dissociating 10-d-old primary neurospheres and replating them in six-well ultra-low binding plates at clonal density. After 10 d, the newly generated (secondary) neurospheres were counted. To reveal multipotency, primary and secondary neurospheres were plated onto polyornithine and fibronectin- or laminin-coated (Sigma) plates and differentiated for 4 d in neurosphere medium supplemented with 2% FBS (ICN Biochemicals). Cells were labeled with antibodies against GFAP (DAKO) and β-tubulin-III (Sigma). Secondary antibodies were FITC-conjugated goat-anti-rabbit and Cy3-conjugated goat-anti-mouse (Jackson ImmunoResearch). Nuclei were stained with DAPI.

Acknowledgments

We thank the Netherlands Cancer Institute FACS and Microscopy Core Facilities for assistance, and G. Hart for advice on statistics. We thank M. Oren for *Mdm2* cDNA, R. DePinho for $Ink4a/Arf^{+/-}$ mice, C. Sherr for $Arf^{+/-}$ mice, A. Berns for $Ink4a^{+/-}$ mice, and L. Donehower for $p53^{+/-}$ mice. We thank J. Deschamps and H. Koseki for $Mel18^{+/-}$ mice, M. Djabali for $M33^{+/-}$ mice, M. Vidal for $Ring1a^{+/-}$ mice, and S. Morrison for sharing unpublished results. S.B., P.S., and J.J. are supported by grants from the Dutch Cancer Society to M.v.L.. M.V.-L. and P.S. are supported by a Pioneer grant from the Netherlands Organization for Scientific Research to M.v.L. S.M. is supported by grants from the Oncosuisse and "Nachwuchsförderung Universität Zürich". Y.A. is supported by the Swiss National Science Foundation, ProVisu, and Velux Foundations, and AFM.

References

Akasaka, T., Kanno, M., Balling, R., Mieza, M.A., Taniguchi, M., and Koseki, H. 1996. A role for mel-18, a Polycomb group-related vertebrate gene, during the anteroposterior specification of the axial skeleton. *Development* **122:** 1513–1522.

Baptista, C.A., Hatten, M.E., Blazeski, R., and Mason, C.A. 1994. Cell–cell interactions influence survival and differentiation of purified Purkinje cells in vitro. *Neuron* **12:** 243–260.

Core, N., Bel, S., Gaunt, S.J., Aurrand-Lions, M., Pearce, J., Fisher, A., and Djabali, M. 1997. Altered cellular proliferation and mesoderm patterning in Polycomb-M33-deficient mice. *Development* **124:** 721–729.

Core, N., Joly, F., Boned, A., and Djabali, M. 2004. Disruption of E2F signaling suppresses the INK4a-induced proliferative defect in M33-deficient mice. *Oncogene* **23:** 7660–7668.

Dahmane, N. and Ruiz-i-Altaba, A. 1999. Sonic hedgehog regulates the growth and patterning of the cerebellum. *Development* **126:** 3089–3100.

De Napoles, M., Mermoud, J.E., Wakao, R., Tang, Y.A., Endoh, M., Appanah, R., Nesterova, T.B., Silva, J., Otte, A.P., Vidal, M., et al. 2004. Polycomb group proteins Ring1A/B link ubiquitylation of histone H2A to heritable gene silencing and X inactivation. *Dev. Cell* **7:** 663–676.

Del Mar Lorente, M., Marcos-Gutierrez, C., Perez, C., Schoorlemmer, J., Ramirez, A., Magin, T., and Vidal, M. 2000. Loss- and gain-of-function mutations show a polycomb group function for Ring1A in mice. *Development* **127:** 5093–5100.

Doetsch, F. 2003. A niche for adult neural stem cells. *Curr. Opin. Genet. Dev.* **13:** 543–550.

Donehower, L.A., Harvey, M., Slagle, B.L., McArthur, M.J., Montgomery Jr., C.A., Butel, J.S., and Bradley, A. 1992. Mice deficient for p53 are developmentally normal but susceptible to spontaneous tumours. *Nature* **356:** 215–221.

Gil, J., Bernard, D., Martinez, D., and Beach, D. 2004. Polycomb CBX7 has a unifying role in cellular lifespan. *Nat. Cell. Biol.* **6:** 67–72.

Haupt, Y., Alexander, W.S., Barri, G., Klinken, S.P., and Adams, J.M. 1991. Novel zinc finger gene implicated as myc collaborator by retrovirally accelerated lymphomagenesis in E μ-myc transgenic mice. *Cell* **65:** 753–763.

Iwama, A., Oguro, H., Negishi, M., Kato, Y., Morita, Y., Tsukui, H., Ema, H., Kamijo, T., Katoh-Fukui, Y., Koseki, H., et al. 2004. Enhanced self-renewal of hematopoietic stem cells mediated by the polycomb gene product Bmi-1. *Immunity* **21:** 843–851.

Jacobs, J.J., Kieboom, K., Marino, S., DePinho, R.A., and van Lohuizen, M. 1999. The oncogene and Polycomb-group gene bmi-1 regulates cell proliferation and senescence through the ink4a locus. *Nature* **397:** 164–168.

Kamijo, T., Zindy, F., Roussel, M.F., Quelle, D.E., Downing, J.R., Ashmun, R.A., Grosveld, G., and Sherr, C.J. 1997. Tumor suppression at the mouse INK4a locus mediated by the alternative reading frame product p19ARF. *Cell* **91:** 649–659.

Kenney, A.M., Cole, M.D., and Rowitch, D.H. 2003. Nmyc upregulation by sonic hedgehog signaling promotes proliferation in developing cerebellar granule neuron precursors. *Development* **130:** 15–28.

Kirmizis, A., Bartley, S.M., Kuzmichev, A., Margueron, R., Reinberg, D., Green, R., and Farnham, P.J. 2004. Silencing of human polycomb target genes is associated with methylation of histone H3 Lys 27. *Genes & Dev.* **18:** 1592–1605.

Krimpenfort, P., Quon, K.C., Mooi, W.J., Loonstra, A., and Berns, A. 2001. Loss of p16Ink4a confers susceptibility to metastatic melanoma in mice. *Nature* **413:** 83–86.

Kuzmichev, A., Jenuwein, T., Tempst, P., and Reinberg, D. 2004. Different EZH2-containing complexes target methylation of histone H1 or nucleosomal histone H3. *Mol. Cell* **14:** 183–193.

Lessard, J. and Sauvageau, G. 2003. Bmi-1 determines the proliferative capacity of normal and leukaemic stem cells. *Nature* **423:** 255–260.

Leung, C., Lingbeek, M., Shakhova, O., Liu, J., Tanger, E., Saremaslani, P., Van Lohuizen, M., and Marino, S. 2004. Bmi1 is essential for cerebellar development and is overexpressed in human medulloblastomas. *Nature* **428:** 337–341.

Lowe, S.W. and Sherr, C.J. 2003. Tumor suppression by Ink4a–Arf: Progress and puzzles. *Curr. Opin. Genet. Dev.* **13:** 77–83.

Molofsky, A.V., Pardal, R., Iwashita, T., Park, I.K., Clarke, M.F., and Morrison, S.J. 2003. Bmi-1 dependence distinguishes neural stem cell self-renewal from progenitor proliferation. *Nature* **425:** 962–967.

Molofsky, A.V., He, S., Bydon, M., Morrison, S.J., and Pardal, R. 2005. Bmi-1 promotes neural stem cell self-renewal and neural development but not mouse growth and survival by repressing the p16^{Ink4a} and p19^{Arf} senescence pathways. *Genes & Dev.* (this issue).

Morshead, C.M., Reynolds, B.A., Craig, C.G., McBurney, M.W., Staines, W.A., Morassutti, D., Weiss, S., and van der Kooy, D. 1994. Neural stem cells in the adult mammalian forebrain: A relatively quiescent subpopulation of subependymal cells. *Neuron* **13:** 1071–1082.

Park, I.K., Qian, D., Kiel, M., Becker, M.W., Pihalja, M., Weissman, I.L., Morrison, S.J., and Clarke, M.F. 2003. Bmi-1 is required for maintenance of adult self-renewing haematopoietic stem cells. *Nature* **423:** 302–305.

Quelle, D.E., Zindy, F., Ashmun, R.A., and Sherr, C.J. 1995. Alternative reading frames of the INK4a tumor suppressor gene encode two unrelated proteins capable of inducing cell cycle arrest. *Cell* **83:** 993–1000.

Reynolds, B.A. and Weiss, S. 1992. Generation of neurons and astrocytes from isolated cells of the adult mammalian central nervous system. *Science* **255:** 1707–1710.

Serrano, M., Hannon, G.J., and Beach, D. 1993. A new regulatory motif in cell-cycle control causing specific inhibition of cyclin D/CDK4. *Nature* **366:** 704–707.

Serrano, M., Lee, H., Chin, L., Cordon-Cardo, C., Beach, D., and DePinho, R.A. 1996. Role of the INK4a locus in tumor suppression and cell mortality. *Cell* **85:** 27–37.

Sharpless, N.E. and DePinho, R.A. 1999. The INK4A/ARF locus and its two gene products. *Curr. Opin. Genet. Dev.* **9:** 22–30.

Sherr, C.J. and Weber, J.D. 2000. The ARF/p53 pathway. *Curr. Opin. Genet. Dev.* **10:** 94–99.

Valk-Lingbeek, M.E. Bruggeman, S.W., and van Lohuizen, M. 2004. Stem cells and cancer: The polycomb connection. *Cell* **118:** 409–418.

Van der Lugt, N.M., Domen, J., Linders, K., van Roon, M., Robanus-Maandag, E., te Riele, H., van der Valk, M., Deschamps, J., Sofroniew, M., and van Lohuizen, M. 1994. Posterior transformation, neurological abnormalities, and severe hematopoietic defects in mice with a targeted deletion of the bmi-1 proto-oncogene. *Genes & Dev.* **8:** 757–769.

Van Lohuizen, M., Verbeek, S., Scheijen, B., Wientjens, E., van der Gulden, H., and Berns, A. 1991. Identification of cooperating oncogenes in E μ-myc transgenic mice by provirus tagging. *Cell* **65:** 737–752.

Voncken, J.W., Roelen, B.A., Roefs, M., de Vries, S., Verhoeven, E., Marino, S., Deschamps, J., and van Lohuizen, M. 2003. Rnf2 (Ring1b) deficiency causes gastrulation arrest and cell cycle inhibition. *Proc. Natl. Acad. Sci.* **100:** 2468–2473.

Wang, V.Y. and Zoghbi, H.Y. 2001. Genetic regulation of cerebellar development. *Nat. Rev. Neurosci.* **2:** 484–491.

Wechsler-Reya, R.J. and Scott, M.P. 1999. Control of neuronal precursor proliferation in the cerebellum by Sonic Hedgehog. *Neuron* **22:** 103–114.

Zencak, D., Lingbeek, M., Kostic, C., Tekaya, M., Tanger, E., Hornfeld, D., Jaquet, M., Munier, F.L., Schorderet, D.F., van Lohuizen, M., et al. 2005. *Bmi1* loss produces an increase in astroglial cells and a decrease in neural stem cell population and proliferation. *J. Neurosci.* (in press).